

ological grouping of the genotypes throughout the epidemic (Fig. 2) (table S2).

In tracing the molecular evolution of SARS-CoV in China, we observed that the epidemic started and ended with deletion events, together with a progressive slowing of the nonsynonymous mutation rates and a common genotype that predominated during the latter part of the epidemic. The mechanistic explanation for the selective adaptation and purification processes that led to such genomic evolutionary changes in SARS-CoV requires further work (29). Nonetheless, this study has provided valuable clues to aid further investigation of this remarkable evolutionary tale.

We have sequenced the complete S gene (GenBank accession number AY525636) from an oropharyngeal swab sample (sampling date, 22 December 2003) collected from the most recent index patient of the city of Guangzhou (onset date, 16 December 2003; hospitalized 20 December 2003; www.wpro.who.int/sars/docs/pressreleases/pr\_27122003.asp). Phylogenetic analysis of this S gene sequence with those from the human SARS-CoV and palm civet SARS-like coronavirus indicated that this most recent case of SARS-CoV is much closer to the palm civet SARS-like coronavirus than to any human SARS-CoV detected in the previous epidemic (fig. S7 and table S4). Because it is evidently different from the recent laboratory infections in Singapore (www.who.int/csr/don/2003\_09\_24/en) and Taiwan (www.who.int/mediacentre/releases/2003/np26/en), it strengthens the argument for animal origin of the human SARS epidemic.

#### References and Notes

- R. A. Fouchier et al., *Nature* **423**, 240 (2003).
- T. G. Ksiazek et al., *N. Engl. J. Med.* **348**, 1953 (2003).
- C. Drosten et al., *N. Engl. J. Med.* **348**, 1967 (2003).
- P. A. Rota et al., *Science* **300**, 1394 (2003).
- M. A. Marra et al., *Science* **300**, 1399 (2003).
- G. Vogel, *Science* **300**, 1062 (2003).
- Y. J. Ruan et al., *Lancet* **361**, 1779 (2003).
- Y. Guan et al., *Science* **302**, 276 (2003).
- S. K. W. Tsui, S. S. C. Chim, Y. M. D. Lo, *N. Engl. J. Med.* **349**, 187 (2003).
- S. S. C. Chim et al., *Lancet* **362**, 1807 (2003).
- R. W. K. Chiu, S. S. C. Chim, Y. M. D. Lo, *N. Engl. J. Med.* **349**, 1875 (2003).
- J. S. Rest, D. P. Mindell, *Infect. Genet. Evol.* **3**, 219 (2003).
- N. S. Zhong et al., *Lancet* **362**, 1353 (2003).
- Supporting materials are available on Science Online.
- K. W. Tsang et al., *N. Engl. J. Med.* **348**, 1977 (2003).
- N. Lee et al., *N. Engl. J. Med.* **348**, 1986 (2003).
- Centers for Disease Control and Prevention, *Morb. Mortal. Wkly. Rep.* **52**, 241 (2003).
- E. J. Snijder et al., *J. Mol. Biol.* **331**, 991 (2003).
- SARS-like coronaviruses were isolated from palm civets farmed domestically in Hubei Province, China, by Hu et al. at the Wuhan Institute of Virology, Chinese Academy of Sciences. Partial genome sequencing revealed an 82-nt deletion within the Orf8 region, which is identical to that found in human SARS-CoV isolates from the early patients of Zhongshan, Guangdong Province, China. Contamination can be ruled out because no human SARS-CoV isolate with the 82-nt deletion has ever been found in that institute or has been isolated in that region of China.
- The SARS-CoV sequence with the 415-nt deletion

- (CUHK-LC2, CUHK-LC3, CUHK-LC4, and CUHK-LC5) was obtained from two SARS patients whose disease was linked to a late cluster of SARS cases in Hong Kong. Both patients had disease onset in mid-May 2003. The CUHK-LC2 sequence was initially obtained from the culture isolate of a throat wash specimen of an infected hospital health care worker and was later confirmed from the same specimen directly. CUHK-LC3, CUHK-LC4, and CUHK-LC5 were obtained from three different nasal swab specimens both directly and from the culture supernatants of an elderly patient who acquired SARS in the same hospital.
- M. M. C. Lai, K. V. Holmes, in *Fields Virology*, D. M. Knipe, P. M. Howley, Eds. (Lippincott Williams & Wilkins, New York, ed. 4, 2001), chap. 35.
- E. G. Brown, H. Liu, L. C. Kit, S. Baird, M. Nesrallah, *Proc. Natl. Acad. Sci. U.S.A.* **98**, 6883 (2001).
- S. H. Seo, E. Hoffmann, R. G. Webster, *Nature Med.* **8**, 950 (2002).
- D. Rasschaert, M. Duarte, H. Laude, *J. Gen. Virol.* **71**, 2599 (1990).
- W.-H. Li, M. Tanimura, P. M. Sharp, *Mol. Biol. Evol.* **5**, 313 (1988).

- J. W. Drake, J. J. Holland, *Proc. Natl. Acad. Sci. U.S.A.* **96**, 13910 (1999).
- Z. Luo, A. M. Matthews, S. R. Weiss, *J. Virol.* **73**, 8152 (1999).
- R. M. Bush, C. B. Smith, N. J. Cox, W. M. Fitch, *Proc. Natl. Acad. Sci. U.S.A.* **97**, 6974 (2000).
- P. W. Ewald, *J. Urban Health* **75**, 480 (1998).
- See SOM Text at Science Online for acknowledgments.

#### Supporting Online Material

www.sciencemag.org/cgi/content/full/1092002/DC1

Materials and Methods

SOM Text

References and Notes

Figs. S1 to S7

Tables S1 to S4

29 September 2003; accepted 14 January 2004

Published online 29 January 2004;

10.1126/science.1092002

Include this information when citing this paper.

## Evidence of a Pluripotent Human Embryonic Stem Cell Line Derived from a Cloned Blastocyst

Woo Suk Hwang,<sup>1,2\*</sup> Young June Ryu,<sup>1</sup> Jong Hyuk Park,<sup>3</sup> Eul Soon Park,<sup>1</sup> Eu Gene Lee,<sup>1</sup> Ja Min Koo,<sup>4</sup> Hyun Yong Jeon,<sup>1</sup> Byeong Chun Lee,<sup>1</sup> Sung Keun Kang,<sup>1</sup> Sun Jong Kim,<sup>3</sup> Curie Ahn,<sup>5</sup> Jung Hye Hwang,<sup>6</sup> Ky Young Park,<sup>7</sup> Jose B. Cibelli,<sup>8</sup> Shin Yong Moon<sup>5\*</sup>

Somatic cell nuclear transfer (SCNT) technology has recently been used to generate animals with a common genetic composition. In this study, we report the derivation of a pluripotent embryonic stem (ES) cell line (SCNT-hES-1) from a cloned human blastocyst. The SCNT-hES-1 cells displayed typical ES cell morphology and cell surface markers and were capable of differentiating into embryoid bodies in vitro and of forming teratomas in vivo containing cell derivatives from all three embryonic germ layers in severe combined immunodeficient mice. After continuous proliferation for more than 70 passages, SCNT-hES-1 cells maintained normal karyotypes and were genetically identical to the somatic nuclear donor cells. Although we cannot completely exclude the possibility that the cells had a parthenogenetic origin, imprinting analyses support a SCNT origin of the derived human ES cells.

The isolation of pluripotent human embryonic stem (ES) cells (1) and breakthroughs in somatic cell nuclear transfer (SCNT) in mammals (2) have raised the possibility of performing human SCNT to generate potentially unlimited sources of undifferentiated

ated cells for use in research, with potential applications in tissue repair and transplantation medicine. This concept, known as "therapeutic cloning," refers to the transfer of the nucleus of a somatic cell into an enucleated donor oocyte (3). In theory, the oocyte's cytoplasm would reprogram the transferred nucleus by silencing all the somatic cell genes and activating the embryonic ones. ES cells would be isolated from the inner cell mass (ICM) of the cloned preimplantation embryo. When applied in a therapeutic setting, these cells would carry the nuclear genome of the patient; therefore, it is proposed that after directed cell differentiation, the cells could be transplanted without immune rejection to treat degenerative disorders such as diabetes, osteoarthritis, and Parkinson's disease

<sup>1</sup>College of Veterinary Medicine, <sup>2</sup>School of Agricultural Biotechnology, Seoul National University, Seoul 151-742, Korea. <sup>3</sup>Medical Research Center, MizMedi Hospital, Seoul, 135-280, Korea. <sup>4</sup>Gachon Medical School, Incheon, 417-840, Korea. <sup>5</sup>College of Medicine, Seoul National University, Seoul, 110-744, Korea. <sup>6</sup>School of Medicine, Hanyang University, Seoul, 471-701, Korea. <sup>7</sup>College of Natural Science, Suncheon National University, Suncheon, 540-742, Korea. <sup>8</sup>Department of Animal Science-Physiology, Michigan State University, East Lansing, MI 48824, USA.

\*To whom correspondence should be addressed. E-mail: hwangws@snu.ac.kr (W.S.H.); shmoo@plaza.snu.ac.kr (S.Y.M.)

## REPORTS

(among others). Previous reports have described the generation of bovine ES-like cells (4) and mouse ES cells from the ICMs of cloned blastocysts (5–7) and the development of cloned human embryos to the 8- to 10-cell stage (8, 9). Here we describe evidence of the derivation of human ES cells after SCNT (10).

Fresh oocytes and cumulus cells were donated by healthy women for the express purpose of SCNT stem cell derivation for therapeutic cloning research and its applications. Before beginning any experiments, we obtained approval for this study from the Institutional Review Board on Human Subjects Research and Ethics Committees (Hanyang University Hospital, Seoul, Korea). Donors were fully aware of the scope of our study and signed an informed consent form (a summary of the informed consent form is available in the supporting online text); donors voluntarily donated oocytes and cumulus cells (including DNA) for therapeutic cloning research and its applications only, not for reproductive cloning; and there was no financial payment. A total of 242 oocytes were obtained from 16 volunteers (there were one or two donors for each trial) after ovarian stimulation: 176 metaphase II (MII) oocytes were used directly for SCNT, whereas the remaining 66 oocytes were allowed to mature to the MII stage before use in SCNT. Autologous SCNT was performed; that is, the do-

nor's own cumulus cell, isolated from the cumulus-oocyte complex (COC), was transferred back into the donor's own enucleated oocyte. Before enucleation, the oocytes were matured in vitro in G1.2 medium (Vitro Life, Goteborg, Sweden) for 1 to 2 hours. Enucleation, SCNT, and electrical fusion were performed as described (11). To directly confirm that the oocyte's DNA was removed during enucleation, we imaged the extruded DNA MII spindle complex from every oocyte with Hoechst 33342 fluorescent DNA dye (Fig. 1, A and B; arrows).

Without any report of an efficient protocol for human SCNT, several critical steps had to be optimized (2), including reprogramming time, activation method, and in vitro culture conditions. Reprogramming time, or the lapse of time between cell fusion and egg activation, returns the gene expression of the somatic cell to that needed for appropriate embryonic development. Initially, we investigated the effect of simultaneous fusion and activation, as used for porcine SCNT (12, 13), but observed low fusion and cleavage rates, with no blastocyst development. Instead, we adapted the bovine SCNT procedure of waiting a few hours between fusion and activation. By allowing 2 hours for reprogramming, we were able to develop ~25% of the embryos to the blastocyst stage.

Because sperm-mediated activation is absent in SCNT, an artificial stimulus is needed to

initiate development. Various chemical, physical, and mechanical agents induce parthenogenetic development in mice (14), but human data are limited. Oocyte activation using the calcium ionophore A23187 (calcimycin) or ionomycin and the protein synthesis inhibitor puromycin induces parthenogenetic development of human oocytes at different efficiencies (15). We found that incubation in 10  $\mu$ M A23187 for 5 min, followed by incubation with 2.0 mM 6-dimethylaminopurine (DMAP) for 4 hours, gave efficient chemical activation for human SCNT eggs. Other investigators have reported encouraging results in overcoming inefficiencies in embryo culture by supplementing the culture with different energy substrates (16). Furthermore, the recent development of serum-free sequential media has led to considerable improvement in the rate of clinical pregnancies produced by in vitro fertilization (IVF) (17). In this study, human modified synthetic oviductal fluid with amino acids (hmSOFaa) was prepared by supplementing mSOFaa (18) with human serum albumin (10 mg/ml) and fructose (1.5 mM) instead of bovine serum albumin (8 mg/ml) and glucose (1.5 mM). The replacement of glucose with fructose improves the developmental competence of bovine SCNT embryos (11, 19). Culture of human SCNT-derived embryos in G1.2 medium for the first 48 hours followed by hmSOFaa medium produced more blastocysts, as compared to culture in G1.2 medium for the first 48 hours followed by culture in G1.2 medium or in continuous hmSOFaa medium (Table 1). Cibelli *et al.* (8) reported that the treatment of human oocytes with 5  $\mu$ M calcium ionomycin followed by 2 mM DMAP in G1.2 culture medium triggered pronucleus formation, embryonic cleavage, and the formation of a blastocoelic cavity in human parthenotes. However, they did not obtain human SCNT blastocysts when their protocol was applied to SCNT embryos. Limitations in oocyte supply precluded full optimization of all the parameters for human SCNT; nonetheless, the protocol described here produced cloned blastocysts at rates of 19 to 29% (as a percentage of oocytes used) and was comparable to those produced by established SCNT methods in cattle (~25%) (11) and pigs (~26%) (12, 13).

A total of 30 SCNT-derived blastocysts were cultured, 20 ICMs were isolated by immunosurgical removal of the trophoblast, and one ES cell line (SCNT-hES-1) was derived. The resulting SCNT-hES-1 cells had a high nucleus-to-cytoplasm ratio and prominent nucleoli. The cell colonies displayed similar morphology to that reported previously for hES cells derived after IVF (Fig. 1, C to E). When cultured in defined medium conditioned for neural cell differentiation (20), SCNT-hES-1 cells differentiated into nestin-positive cells, an indication of primitive neuroectoderm differentiation (Fig. 1F). The SCNT-hES-1 cell line was mechanically passaged by dissociation every 5 to 7 days and successfully maintained its undifferentiated mor-

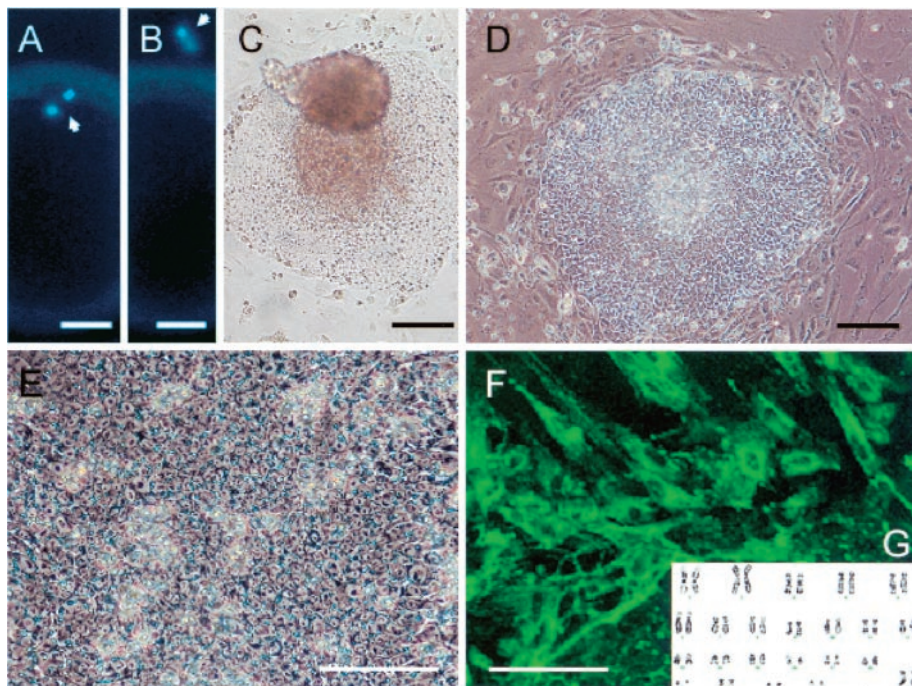


**Fig. 1.** Confirmation of enucleation, photographs of human SCNT ES cells and their differentiated progeny, and karyotype analysis. (A and B) Images ( $\times 200$ ) of extruded DNA MII spindle complexes (arrows) from an oocyte before (A) and after (B) enucleation. (C to E) Bright-field [(C),  $\times 100$ ] and phase contrast [(D),  $\times 100$ ] micrographs and higher magnification image [(E),  $\times 200$ ] of a colony of SCNT-hES-1 cells. Immunofluorescence staining for nestin [(F),  $\times 200$ ] and G-banded karyotyping (G) in SCNT-hES-1 cells are shown. Scale bars, 20  $\mu$ m in (A) and (B) and 100  $\mu$ m in (C) to (F).

phology after continuous proliferation for >70 passages, while still maintaining a normal female (XX) karyotype (Fig. 1G) (21). Furthermore, the SCNT-hES-1 cells expressed ES cell markers such as alkaline phosphatase, SSEA-3, SSEA-4, TRA-1-60, TRA-1-81, and Oct-4, but not SSEA-1 (Fig. 2). As previously described in monkey (22) and human ES cells (1, 23, 24) and in mouse SCNT-ES cells (6), SCNT-hES-1 cells did not respond to exogenous leukaemia inhibitory factor, suggesting that a pluripotent state is maintained by a gp130-independent pathway. The pluripotency of SCNT-hES-1 cells was investigated in vitro (fig. S1) and in vivo (Fig. 3). Clumps of the cells were cultured in vitro in suspension to form embryoid bodies. The resulting embryoid bodies were stained with three dermal markers and were found to differentiate into a variety of cell types, including derivatives of endoderm, mesoderm, and ectoderm (fig. S1). When undifferentiated SCNT-hES-1 cells were injected into the testes of severe combined immunodeficient (SCID) mice, teratomas were obtained 6 to 7 weeks after injection. The resulting teratomas contained tissue representative of all three germ layers. Differentiated tissues seen in Fig. 3 include neuroepithelial rosettes, pigmented retinal epithelium, smooth muscle, bone, cartilage, connective tissues, and glandular epithelium. The DNA fingerprinting analysis with human short tandem repeat (STR) markers indicates that the cell line originated from the cloned blastocysts reconstructed from the donor cells, not from parthenogenetic activation (Fig. 4, A to C). The statistical probability that the cells may have derived from an unrelated donor is  $8.8 \times 10^{-16}$ . Reverse transcription polymerase chain reaction (RT-PCR) amplification for paternally expressed (*hSNRPN* and *ARHI*) and maternally expressed (*UBE3A* and *H19*) genes further confirmed that the cell line originated from the donor cells (Fig. 4D).

Simerly *et al.* (26) recently reported defective mitotic spindles after SCNT in nonhuman primate embryos, perhaps resulting from the depletion of microtubule motor and centrosome proteins lost to the meiotic spindle after enucleation. In this study, Fig. 1G demonstrates that SCNT-hES-1 cells have the normal karyotype. We speculate that SCNT blastocysts from which ES cell lines were not derived might have been aneuploid. However, it is important to note that our investigations differ from those of Simerly *et al.* in a few ways: Media and protocols for in vitro development were optimized for human oocytes and embryos, whereas the protocols for nonhuman primate studies are extrapolated from clinical procedures; the enucleation method here differs, because we squeeze the MII oocyte so that the DNA spindle complex is extruded through a small hole in the zona pellucida, instead of aspirating the DNA spindle complex with a

glass pipette as others have described (27); and the DNA spindle complex is extruded shortly after the appearance of the first polar body, so that it may even be at the prometaphase II stage.

In this report, we provide three lines of

evidence supporting the nuclear transfer origins of the SCNT-hES-1 cell line: (i) DNA extraction was verified for each of the 242 enucleated oocytes (Fig. 1, A and B; arrows); (ii) DNA fingerprinting showed heterozy-

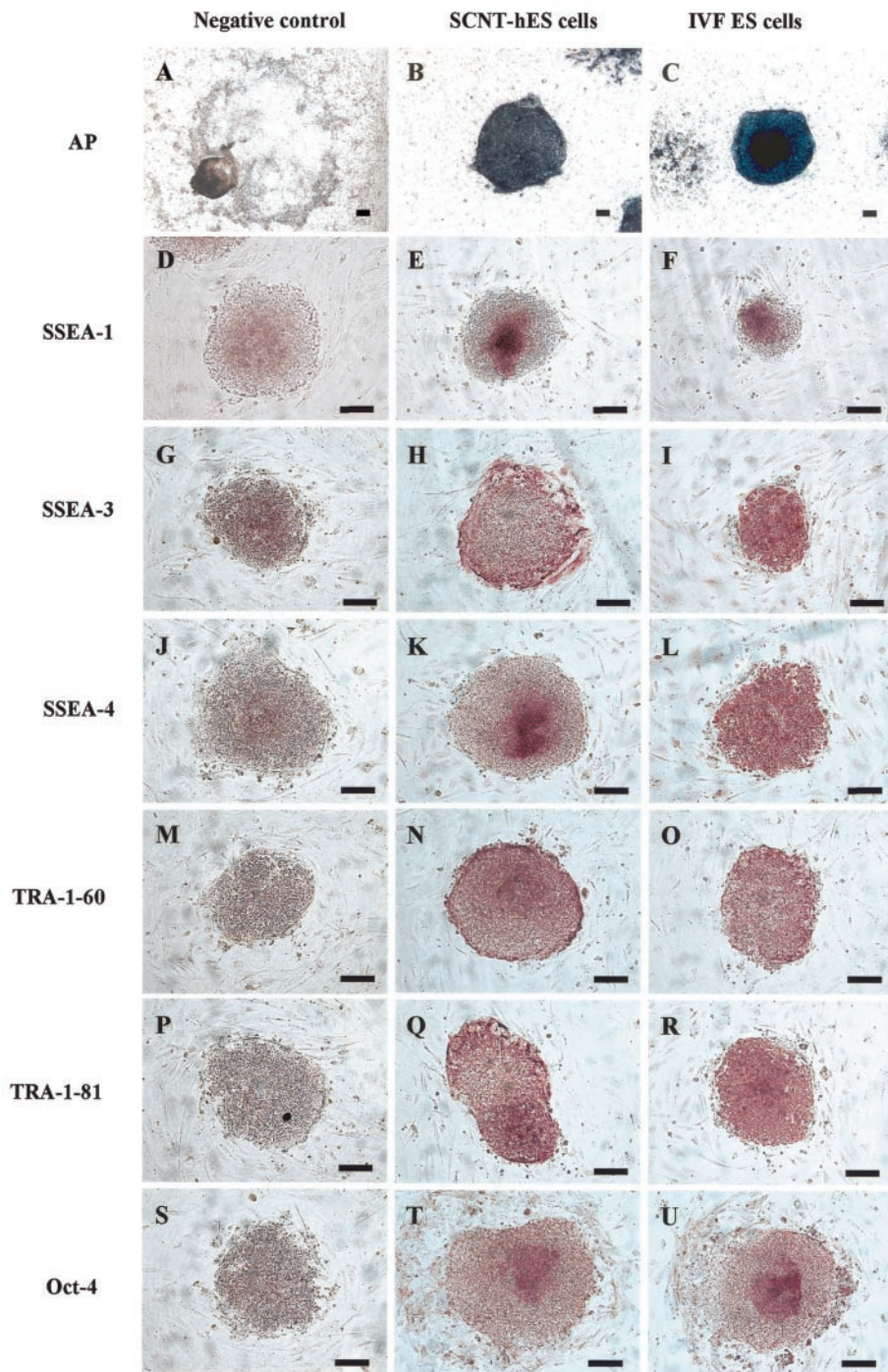


**Fig. 2.** Expression of characteristic cell surface markers in human SCNT ES cells. SCNT-hES-1 cells expressed cell surface markers, including alkaline phosphatase (B), SSEA-3 (H), SSEA-4 (K), TRA-1-60 (N), TRA-1-81 (Q), and Oct-4 (T), but not SSEA-1 (E). The differentiated SCNT-hES-1 cells were not stained with alkaline phosphatase (A). The IVF-derived human ES cells (Miz-hES) were used for comparison and also expressed alkaline phosphatase (C), SSEA-3 (I), SSEA-4 (L), TRA-1-60 (O), TRA-1-81 (R), and Oct-4 (U), but not SSEA-1 (F). Negative controls not treated with first antibodies are shown (D, G, J, M, P, and S). Magnification in (A) to (U),  $\times 40$ . Scale bars, 100  $\mu\text{m}$ .

## REPORTS

gous, not homozygous, chromosomes (Fig. 4, A to C); and (iii) RT-PCR showed biparental, and not unimaternal, expression of imprinted genes (Fig. 4D). Although the Cyno-1 parthenogenetic cells retained their strictly maternal imprints, that evidence came from a single monkey cell line. Given the aberrant expression of imprinted genes after murine SCNT (28), perhaps the SCNT-hES-1 cells' biparental expression of imprinted genes might have been influenced by SCNT or subsequent culture. Heterologous along with autologous SCNT will provide more definitive molecular evidence. Although overwhelming ethical constraints preclude any reproductive cloning attempts, complementary investigations in nonhuman primates might provide additional and confirmatory information. Consequently, although we cannot exclude the possibility of a parthenogenetic origin, the studies reported here support the conclusion that the SCNT-hES-1 cell line originated from the donor's diploid somatic cumulus cell after SCNT.

In order to successfully derive immunocompatible human ES cells from a living donor, a reliable and efficient method for producing cloned embryos and ES isolation must be developed. Thomson *et al.* (1), Reubinoff *et al.* (23), and Lanzendorf *et al.* (29) produced human ES cell lines at high efficiency. Briefly, five ES cell lines were derived from a total of 14 ICMs, two ES cell lines were derived from four ICMs, and three ES cell lines were derived from 18 ICMs, respectively. In our study, one SCNT-hES cell line was derived from 20 ICMs. It

remains to be determined whether this low efficiency is due to faulty reprogramming of the somatic cells or to subtle variations in our experimental procedures. We cannot rule out the

possibility that the genetic background of the cell donor had an impact on the overall efficiency of the procedure. Further improvements in SCNT protocols and in vitro culture

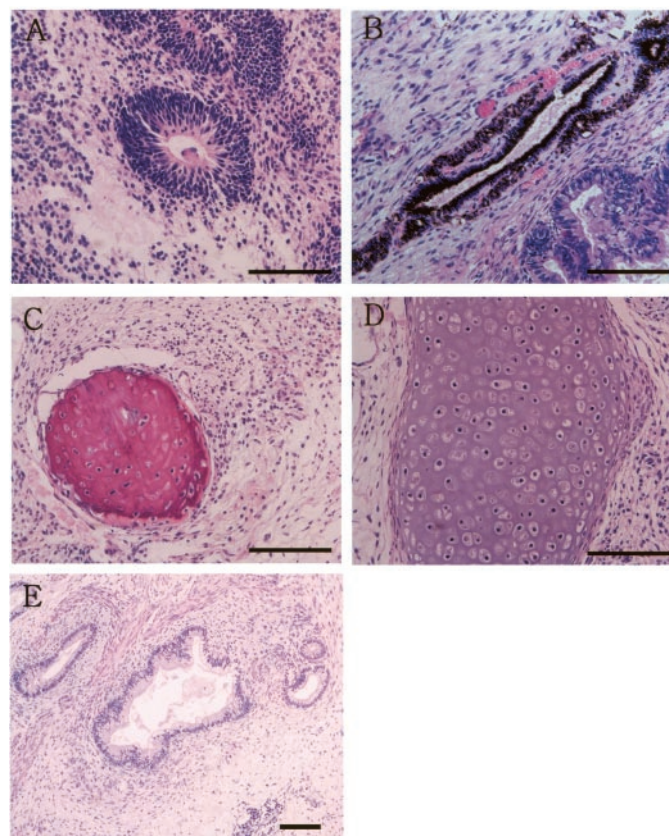


**Fig. 3.** Teratomas formed by human SCNT ES cells in the testes of SCID mice at 12 weeks after injection. Neuroepithelial rosette (A), pigmented retinal epithelium (B), ostoid island showing bony differentiation (C), cartilage (D), and glandular epithelium with smooth muscle and connective tissues (E). Magnification in (A) to (D),  $\times 200$ ; in (E),  $\times 100$ . Scale bar, 100  $\mu\text{m}$ .

**Table 1.** Conditions for human SCNT.

Experiment	Activation condition*		Reprogramming time (hours)	1st step medium†	2nd step medium	No. of oocytes	No. (%) of cloned embryos developed to		
							Two-cell	Compacted morula	Blastocyst
1st set	10 $\mu\text{M}$ ionophore	6-DMAP	2	G 1.2	hmSOFaa	16	16 (100)	4 (25)	4 (25)
	10 $\mu\text{M}$ ionophore	6-DMAP	4	G 1.2	hmSOFaa	16	15 (94)	1 (6)	0
	10 $\mu\text{M}$ ionophore	6-DMAP	6	G 1.2	hmSOFaa	16	15 (94)	1 (6)	1 (6)
	10 $\mu\text{M}$ ionophore	6-DMAP	20	G 1.2	hmSOFaa	16	9 (56)	1 (6)	0
2nd set	10 $\mu\text{M}$ ionophore	6-DMAP	2	G 1.2	hmSOFaa	16	16 (100)	5 (31)	3 (19)
	5 $\mu\text{M}$ ionophore	6-DMAP	2	G 1.2	hmSOFaa	16	11 (69)	0	0
	10 $\mu\text{M}$ ionomycin	6-DMAP	2	G 1.2	hmSOFaa	16	12 (75)	0	0
	5 $\mu\text{M}$ ionomycin	6-DMAP	2	G 1.2	hmSOFaa	16	9 (56)	0	0
3rd set	10 $\mu\text{M}$ ionophore	6-DMAP	2	G 1.2	hmSOFaa	16	16 (100)	4 (25)	3 (19)
	10 $\mu\text{M}$ ionophore	6-DMAP	2	G 1.2	G 2.2	16	16 (100)	0	0
	10 $\mu\text{M}$ ionophore	6-DMAP	2	Continuous	hmSOFaa	16	16 (100)	0	0
4th set	10 $\mu\text{M}$ ionophore	6-DMAP	2	G 1.2	hmSOFaa	66	62 (93)	24 (36)	19 (29)

\*Fused donor oocytes and somatic cells were activated in either calcium ionophore A23187 (5 or 10  $\mu\text{M}$ ) or ionomycin (5 or 10  $\mu\text{M}$ ) for 5 min, followed by 2 mM 6-DMAP treatment for 4 hours. †Oocytes were incubated in the first medium for 48 hours.

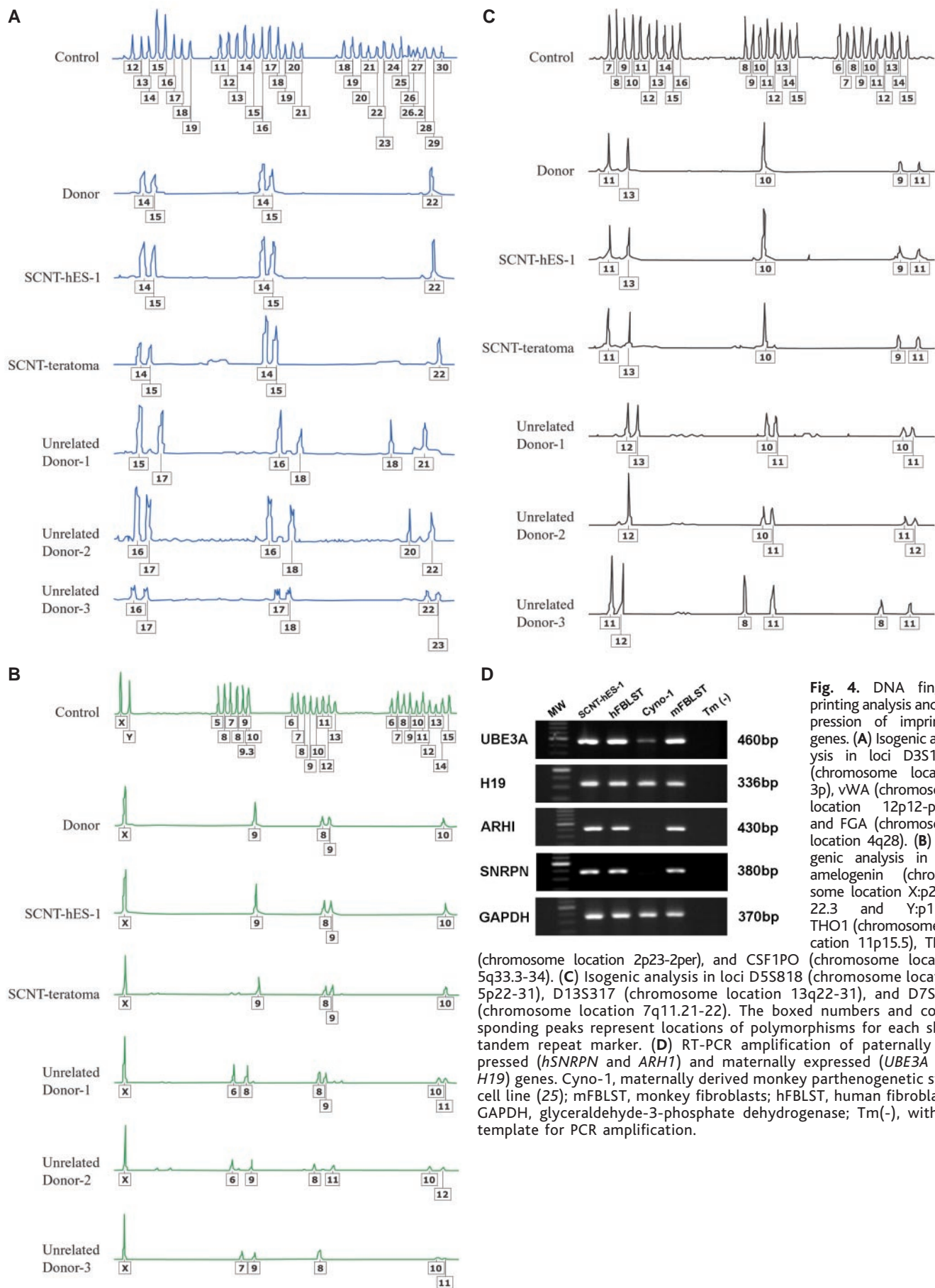


**Fig. 4.** DNA fingerprinting analysis and expression of imprinted genes. **(A)** Isogenic analysis in loci D3S1358 (chromosome location 3p), vWA (chromosome location 12p12-pter), and FGA (chromosome location 4q28). **(B)** Isogenic analysis in loci amelogenin (chromosome location X:p22.1-22.3 and Y:p11.2), THO1 (chromosome location 11p15.5), TPOX (chromosome location 2p23-2per), and CSF1PO (chromosome location 5q33.3-34). **(C)** Isogenic analysis in loci D5S818 (chromosome location 5p22-31), D13S317 (chromosome location 13q22-31), and D7S820 (chromosome location 7q11.21-22). The boxed numbers and corresponding peaks represent locations of polymorphisms for each short tandem repeat marker. **(D)** RT-PCR amplification of paternally expressed (*UBE3A* and *ARHI*) and maternally expressed (*UBE3A* and *H19*) genes. Cyno-1, maternally derived monkey parthenogenetic stem cell line (25); mFBLST, monkey fibroblasts; hFBLST, human fibroblasts; GAPDH, glyceraldehyde-3-phosphate dehydrogenase; Tm(-), without template for PCR amplification.

systems are needed before contemplating the use of this technique for cell therapy. In addition, the mechanisms governing the differentiation of human tissues must be elucidated in order to produce tissue-specific cell populations from undifferentiated ES cells. This study shows the feasibility of generating human ES cells from a somatic cell isolated from a living person.

References and Notes

1. J. A. Thomson *et al.*, *Science* **282**, 1145 (1998).
2. D. Solter, *Nature Rev. Genet.* **1**, 199 (2000).
3. R. P. Lanza, J. B. Cibelli, M. D. West, *Nature Med.* **5**, 975 (1999).
4. J. B. Cibelli *et al.* *Nature Biotechnol.* **16**, 642 (1998).
5. M. J. Munsie *et al.*, *Curr. Biol.* **10**, 989 (2000).
6. E. Kawase, Y. Yamazaki, T. Yagi, R. Yanagimachi, R. A. Pederson, *Genesis* **28**, 156 (2000).
7. T. Wakayama *et al.*, *Science* **292**, 740 (2001).
8. J. B. Cibelli *et al.*, *J. Regen. Med.* **26**, 25 (2001).
9. Y. Shu, G. Zhuang, *Fertil. Steril.* **78**, S286 (2002).
10. Materials and methods are available as supporting material on Science Online.
11. J. Kwun *et al.*, *Mol. Reprod. Dev.* **65**, 167 (2003).
12. S. H. Hyun *et al.*, *Biol. Reprod.* **69**, 1060 (2003).

13. B. Kuhholzer, R. J. Hawley, L. Lai, D. Kolber-Simonds, R. S. Prather, *Biol. Reprod.* **64**, 1635 (2004).
14. M. H. Kaufman, *Nature* **242**, 475 (1973).
15. K. Nakagawa *et al.*, *Zygote* **9**, 83 (2001).
16. D. K. Gardner, M. Lane, W. B. Schoolcraft, *J. Reprod. Immunol.* **55**, 85 (2002).
17. A. Langendonck, D. Demylle, C. Wyns, M. Nisolle, J. Donnez, *Fertil. Steril.* **76**, 1023 (2001).
18. Y. H. Choi, B. C. Lee, J. M. Lim, J. M. S. K. Kang, W. S. Hwang, *Theriogenology* **58**, 1187 (2002).
19. D. K. Barnett, B. D. Bavister, *Mol. Reprod. Dev.* **43**, 105 (1996).
20. S. H. Lee, N. Lumelsky, L. Studer, J. M. Auerbach, R. D. Mckay, *Nature Biotechnol.* **18**, 675 (2000).
21. F. Mitelman, *An International System for Human Cytogenetic Nomenclature* (S. Karger, Basel, Switzerland, 1995).
22. J. A. Thomson *et al.*, *Proc. Natl. Acad. Sci. U.S.A.* **92**, 7844 (1995).
23. B. E. Reubinoff, F. P. Pera, C.-Y. Fong, A. Trounson, A. Bongso, *Nature Biotechnol.* **18**, 399 (2000).
24. S. R. John, *Trends Biotechnol.* **20**, 417 (2002).
25. K. E. Vrana *et al.*, *Proc. Natl. Acad. Sci. U.S.A.* **100** (suppl. 1), 1911 (2003).
26. C. Simerly *et al.*, *Science*, **300**, 297 (2003).
27. I. Wilmut *et al.*, *Nature* **385**, 810 (1997).
28. D. Humphreys *et al.*, *Proc. Natl. Acad. Sci. U.S.A.* **99**, 12889 (2002).
29. S. E. Lanzendorf *et al.*, *Fertil. Steril.* **76**, 132 (2001).
30. We thank Y. Y Hwang (Hanyang University) for assistance with oocyte collections; S. I. Rho (MizMedi

Hospital), H. S. Yoon (MizMedi Hospital,) and S. K. Oh (Seoul National University) for assistance on hES cells culture; Y. K. Choi (Korea Research Institute of Bioscience and Biotechnology) for assistance on teratoma formation; Tak Ko (Michigan State University) for gene expression analysis of Cyno-1 cells; and A. Trounson (Monash University), B. D. Bavister (University of New Orleans), and D. P. Wolf (Oregon National Primate Research Center) for critical review of the manuscript. J. B. Cibelli made intellectual contributions to the manuscript and the RNA analysis of nonhuman primate cells. All human experiments were performed in Korea by Korean scientists. This study was supported by grants from Advanced Backbone IT Technology Development (grant IMT2000-C1-1) to W.S.H. and the Stem Cell Research Center (grant M102KLO100-02K1201-00223) to S.Y.M. The authors are grateful for a graduate fellowship provided by the Ministry of Education through the BK21 program.

Supporting Online Material

www.sciencemag.org/cgi/content/full/1094515/DC1  
 Materials and Methods  
 SOM Text  
 Fig. S1

9 December 2003; accepted 4 February 2004

Published online 12 February 2004;  
 10.1126/science.1094515

Include this information when citing this paper.

# Force-Clamp Spectroscopy Monitors the Folding Trajectory of a Single Protein

Julio M. Fernandez\* and Hongbin Li

We used force-clamp atomic force microscopy to measure the end-to-end length of the small protein ubiquitin during its folding reaction at the single-molecule level. Ubiquitin was first unfolded and extended at a high force, then the stretching force was quenched and protein folding was observed. The folding trajectories were continuous and marked by several distinct stages. The time taken to fold was dependent on the contour length of the unfolded protein and the stretching force applied during folding. The folding collapse was marked by large fluctuations in the end-to-end length of the protein, but these fluctuations vanished upon the final folding contraction. These direct observations of the complete folding trajectory of a protein provide a benchmark to determine the physical basis of the folding reaction.

Resolving the folding pathway of a protein remains a challenge in biology (1–9). Here, we demonstrate a method by which the entire folding trajectory of a single protein can be recorded as a function of time. We used single-molecule atomic force microscopy techniques (10, 11) in the force-clamp mode (12, 13) to apply a constant force to a single polyprotein composed of nine repeats of the small protein ubiquitin (13–16). This resulted in the probabilistic unfolding of ubiquitin, which was observed as stepwise elongations of the protein in which each step correspond-

ed to the unfolding of an individual protein module (12). We applied this technique to monitor the end-to-end length of a single ubiquitin polyprotein (17) during reversible unfolding-folding cycles. Our experimental approach is illustrated in Fig. 1. Figure 1A shows the changes in the length of a single ubiquitin polyprotein in response to the stretching force displayed in Fig. 1B. As shown, stretching the polyubiquitin chain at 120 pN triggers a series of unfolding events that appear as a staircase of 20-nm steps, marking the unfolding of the individual ubiquitins in the chain (Fig. 1A). After 4 s, the force was relaxed to 15 pN (Fig. 1B) (18), and we observed the protein spontaneously contract in stages until it reached its folded length (Fig. 1A). To confirm that the polypro-

tein had folded, we raised the stretching force back to 120 pN at 14 s (Fig. 1B) and observed the ubiquitin chain extend in steps of 20 nm back to its fully unfolded length (Fig. 1A). Hence, the spontaneous contraction of the protein observed upon reducing the force from 120 pN down to 15 pN corresponds to the folding trajectory of the mechanically unfolded ubiquitin.

We observed and analyzed 81 folding events similar to those shown in Fig. 1. Two typical folding trajectories for mechanically unfolded polyubiquitin molecules are shown in Fig. 2. Most of the folding trajectories are qualitatively similar, following a continuous convex time course marked by abrupt changes in slope. However, we have never observed identical sets of trajectories, indicating the existence of multiple folding pathways for ubiquitin. To simplify the analysis of the folding trajectories, we divided their time course, roughly, into four distinct stages marked by abrupt changes in the slope of the collapse (Fig. 2). As an example, we analyze the recording shown in Fig. 2A. The first stage (1 in Fig. 2A and inset) is fast, lasting ~10 ms, which is slower than the time it takes the force to reach its set point (~3 ms in this experiment). The collapse rate for this stage ( $cr_1 = 2135$  nm/s) is within the range but clearly slower than the maximum rate of change, or slew rate ( $sr$ ), of the feedback during this experiment (measured at  $sr = \sim 8300$  nm/s, after the molecule detached from the cantilever). This stage is likely to correspond to the elastic recoil of the unfolded polypeptide chain adjusting its length to the step change in the pulling force. This stage is always fast and is clearly marked in

Department of Biological Sciences, Columbia University, New York, NY 10027, USA.

\*To whom correspondence should be addressed. E-mail: jfernandez@columbia.edu

# ERRATUM

post date 16 December 2005

**Reports:** "Evidence of a pluripotent human embryonic stem cell line derived from a cloned blastocyst" by W. S. Hwang *et al.* (12 Mar. 2004, p. 1669). Contrary to the statements in the second paragraph of text and first paragraph of the supporting online material, which indicated that there was no financial payment to oocyte and cumulus cell donors, some oocyte donors were financially compensated for their donation with a payment of approximately U.S. \$1,400.